Preparation and characterization of cationic nanofibrillated cellulose from etherification and high-shear disintegration processes

T. T. T. Ho · T. Zimmermann · R. Hauert · W. Caseri

Abstract Oat straw cellulose pulp was cationized in an etherification reaction with chlorocholine chloride. The cationized cellulose pulp was then mechanically disintegrated in two process steps to obtain trimethylammonium-modified nanofibrillated cellulose (TMA-NFC). The materials thus obtained were analyzed by elemental analysis, X-ray photoelectron spectroscopy (XPS), X-ray diffraction (XRD), scanning electron microscopy (SEM) and other techniques. A higher nitrogen content of TMA-NFC samples was found by XPS analysis than by elemental analysis, which indicates that the modification occurred mainly on the surface of cellulose fibrils. XPS also confirmed the existence of ammonium groups in the samples. SEM provided images of very fine network structures of TMA-NFC, which affirmed the positive effect of ionic charge on mechanical disintegration process. According to XRD and SEM results, no severe degradation of the cellulose occurred, even at high reaction temperatures. Because of the different properties of the cationic NFC compared to negatively charged native cellulose fibers, TMA-NFC may find broad applications in technical areas, for instance in combination with anionic species, such as fillers or dyes. Indeed, TMA-NFC seems to improve the distribution of clay fillers in NFC matrix.

T. T. T. Ho (✉) · T. Zimmermann
Empa, Swiss Federal Laboratories for Materials Science and Technology, Wood Laboratory, Duebendorf, Switzerland
e-mail: thuthao.ho@empa.ch

R. Hauert
Empa, Swiss Federal Laboratories for Materials Science and Technology, Laboratory for Nanoscale Materials Science, Duebendorf, Switzerland

W. Caseri
ETH, Swiss Federal Institute of Technology, Institute for Polymer, Zurich, Switzerland

Introduction

Cellulose is a polysaccharide composed of D-anhydroglucopyranose units joined by β-1,4-glucosidic bonds. It is the most abundant renewable natural polymer on earth which serves as a primary reinforcing component in plant structures and makes up almost 50% of wood. Due to an increasing demand for environmental-friendly and biocompatible products in various applications, such as medicine, cosmetics, automotive industry, textile, or packaging, cellulose-based materials are in the focus of numerous studies. As cellulose belongs to natural fibers, it is associated with renewability and biodegradability. Further, it is

characterized by non-abrasiveness, low density and low cost (Azizi Samir et al. 2005; Bledzki and Gassan 1999).

In plant cell walls, cellulose exists as a system of fibrils associated by hydrogen bonds. In cellulose fibrils, highly ordered and disordered regions exist alternately, namely as crystalline and amorphous phases. By treating the cell walls chemically, enzymatically or mechanically, it is possible to isolate smaller or wider cellulose fibril aggregates. From such disintegration processes, nanofibrillated cellulose (NFC) is obtained. Ionic charges of cellulose could facilitate the isolation of nanofibrillated cellulose (Wagberg et al. 2008; Eyholzer et al. 2010). Diameters of isolated cellulose fibril aggregates are usually below 100 nm with lengths in the micrometer range. Therefore they exhibit aspect ratios of at least 50–100 (Turbak et al. 1983; Zimmermann et al. 2004; Tanem et al. 2006; Hubbe et al. 2008). The cellulose fibrils are aligned in diverse angles within the cell wall, but after isolation they form entangled network structures due to strong hydrogen bonding between hydroxyl groups.

Compared to native cellulose fibers, NFC shows a much higher grade of homogeneity, higher tensile strength and modulus, smaller fiber sizes (higher aspect ratios), high quantity of reactive surface –OH groups per mass unit of cellulose due to larger specific surface area, high crystallinity levels, and higher transparency (Hubbe et al. 2008; Siró and Plackett 2010; Eichhorn et al. 2010). Many studies reported that NFC can act as a reinforcing component in polymer composites (Iwamoto et al. 2005; Nogi et al. 2005; Sorrentino et al. 2007; Zimmermann et al. 2005; Eichhorn et al. 2010; Hubbe et al. 2008; Cheng et al. 2007; Tingaut et al. 2009; Siqueira et al. 2009; Siró and Plackett 2010). Especially the strength and stiffness of water-soluble polymers can be increased significantly by addition of NFC. For instance, composites of poly(vinyl alcohol) and 10% w/w NFC or of hydroxypropyl cellulose and 20% w/w NFC possess moduli of elasticity which are 3 times higher compared to that of the neat polymer (Zimmermann et al. 2004). However, increased stiffness and decreased damping values were also reported for composites of NFC with apolar polymers like polypropylene, poly(lactic acid) and poly(caprolactone) (Cheng et al. 2007; Tingaut et al. 2009; Siqueira et al. 2009). Further, NFC could also improve barrier properties due to its relatively high crystallinity (Aulin et al.

2009) in combination with the ability of NFC to form a dense network (Fendler et al. 2007; Syverud and Stenius 2009).

Commonly, cellulose fibers are negatively charged due to the presence of –O⁻ and –COO⁻ groups which arise from deprotonation of alcohol or small amounts of carboxylic acid groups, respectively. The anionic surface charges of cellulose fibers repel other anionic materials such as inorganic fillers or anionic dyes which are extensively used in paper-making or textile industry. Hence, cationized cellulose is used to facilitate the dispersion of fillers or dyes. In paper-making industry, the homogeneous dispersion of filler particles, for instance clay platelets, in cellulose fiber networks is expected to improve the mechanical properties of the composites as well as to provide end-use functions for paper products. In textile industry, improvement of dye retention or cellulose dyeability through cationization of cellulose should help to solve an environmental issue resulting from otherwise high concentrations of electrolytes needed in dye baths; and, certainly, to enhance the effectiveness of the dyeing processes. Cationized cellulose is also used to react with anionic dyes from waste in dyeing industry (Abbott et al. 2006). Besides, cationic cellulose is an ideal polymer used in moisturizers and conditioners in cosmetics industry (Peffly et al. 2004; Daly et al. 2010). Moreover, cationic cellulose with quaternary ammonium groups has antibacterial properties (Roy et al. 2007) which could be utilized in food packaging or sanitary materials. Due to these important industrial applications, cationized cellulose is subject of the work described in the following.

Some authors reported the cationization of cellulose; however, the available literature on this topic is relatively rare. Cationization by absorption of a cationic polyelectrolyte like polyethylenimine (PEI), polydiallyldimethylammonium chloride (PDADMAC) or polyallylamine hydrochloride (PAH) (Alince et al. 1991; de la Orden et al. 2007; Wagberg et al. 2008) on cellulose exhibits some disadvantages. For example, polyelectrolytes possibly bind cellulose fibers together which, in most cases, will cause agglomeration. Further, polyelectrolytes only physically adsorb on fiber surfaces, which implies that the interaction between cellulose fibers and polyelectrolyte is probably less sustainable than in chemical modifications. There are few ways of introduction of cationic groups in cellulose by chemical reaction.
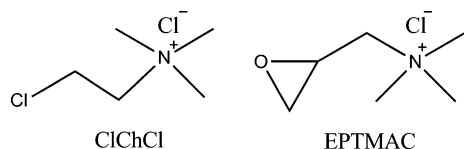
Fig. 1 Chemical structures of ClChCl and EPTMAC

For instance, attaching quaternary ammonium groups by use of 2,3-epoxypropyl trimethylammonium chloride (EPTMAC, Fig. 1) (Cai et al. 2003; Hasani et al. 2008; Montazer et al. 2007) or conversion with hexamethylene diisocyanate followed by reaction with amines (Stenstad et al. 2008). Conversion with EPTMAC provides positive ionic charges to cellulose but uncontrollable side reactions also proceed (Hasani et al. 2008). This is as well the case in reactions with diisocyanates, where isocyanate groups react with hydroxyl groups to form urethane bonds which subsequently react continuously with isocyanates and where crosslinking can occur due to the bifunctionality of the diisocyanate. In 2006, Abbott et al. (2006) reported a cationization reaction of cotton with chlorocholine chloride (ClChCl, Fig. 1). In contrast to EPTMAC, undesired side reactions do not proceed with ClChCl. Ionic liquids were used as solvent and reagent, which is, however, not applicable in industrial conditions because of huge consumption of the expensive ionic liquids per gram of cellulose. Also, the obtained materials had not been thoroughly characterized.

Most of the above mentioned studies on cationized cellulose were performed with fibers while nanofibrillated cellulose has hardly been considered. Therefore, in this article, a process to obtain cationized nanofibrillated cellulose is described, by means of ClChCl, notably without application of ionic liquids. The NFC thus obtained, contained trimethylammonium groups and is therefore designated as TMA-NFC. These materials were characterized with various methods, and it was also shown that TMA-NFC improved the dispersibility of clay in cellulose.

Experimental

Materials

Cellulose pulp powder produced from oat straw with a hemicellulose content of 22.6 and 0.2% rest lignin (Jelucel OF300, Rosenberg, Germany) was used as starting raw material. Chlorocholine chloride (ClChCl) was supplied by Zhengzhou Nongda Biochemical Products Plant (China). Sodium hydroxide (NaOH) was purchased from Fluka (Switzerland). Cellulose pulp powder, ClChCl and NaOH were dried over vacuum at 0.18 mbar overnight at room temperature prior to further processing. Dimethyl sulfoxide (DMSO) was bought from Roth (Switzerland) and dried over 4A molecular sieve for 2 days just before use, ethylacetate from Merck (Germany), methanol (MeOH) from Thommen-Furler AG (Switzerland) and methylene blue (3,9-bisdimethylaminophenazothionium chloride) (MB) from Fluka (Switzerland).

The applied clay was montmorillonite EXM 1246 from Süd-Chemie AG (Germany) with a cation exchange capacity of 106 milliequivalents/100 g. The employed water was of deionized quality.

Chemical modification

In a typical experiment, 5 g of cellulose pulp and 200 mL of DMSO were introduced in a 500 mL three-necked round-bottomed flask equipped with an air condenser and a mechanical stirrer (RW 16 basic, IKA Werke). The mixture was stirred under N_2 atmosphere for 11 h to swell the cellulose.

Different amounts of NaOH and ClChCl, as well as various temperatures and reaction times were evaluated. The NaOH content was varied from 2 to 7 hydroxide ions per alcohol group of cellulose, the ClChCl content also from 2 to 7 ClChCl molecules per alcohol group of cellulose, the temperature from 60 to 120 °C and the reaction time from 8 to 28 h. The products from two reaction conditions (see Table 1)

Table 1 Reaction conditions applied for the chemical modification of cellulose

	Reaction temperature 97.5 °C	Reaction temperature 120 °C
ChClCh[a] (ratio[c])	4.5	4.6
NaOH[b] (ratio[c])	5	2
Time (h)	20	20

[a] ClChCl was dispersed in DMSO (stock solution ca. 30 g of ClChCl in 100 mL of DMSO)

[b] NaOH was dispersed in DMSO (stock solution ca. 10 g of NaOH in 50 mL of DMSO)

[c] The ratios refer to the equivalents of the respective compound to –OH groups in cellulose pulp

were chosen for further characterization and processing steps.

The respective quantities of NaOH and ClChCl were dispersed in DMSO (see also Table 1), respectively, by using a homogenizer (Ultra-turrax T25 digital, IKA Werke). First, the NaOH/DMSO suspension was transferred under stirring into the reaction flask containing the cellulose pulp/DMSO suspension. Thereafter, the ClChCl/DMSO suspension was added and the reaction mixture was heated subsequently to the respective temperatures (Table 1) for 20 h. After cooling to room temperature, the reaction mixture was centrifuged (Hettich Laborapparate, Switzerland) in order to separate excess DMSO. The sediment was washed with ethylacetate to remove DMSO. Subsequently, MeOH and MeOH/H₂O (10/9 v/v) were used in order to remove the by-product choline chloride. Finally, the product was washed 3 times with deionized water to remove NaCl and traces of other used solvents. 200 mL of solvent was used for each washing step. The resulting modified cellulose was stored in 500 mL of water, and subsequently disintegrated to obtain modified NFC suspensions.

Mechanical disintegration

The disintegration process of NFC from the cellulose pulp powder is the combination of two mechanical treatment processes using an inline dispersing system (Megatron MT 3000, Kinematica AG, Switzerland) for pre-treatment and a high pressure homogenizer (lab-scale Microfluidizer type M-110Y, Microfluidics Corporation, USA) for disintegration of the cellulose material.

In the first process step, 80 g of starting material cellulose pulp powder was dispersed in 8 L of water in a 10-L thermo-static reactor (swollen for at least 5 days). After this time, the swollen cellulose suspension was passed through a closed inline dispersing system equipped with an ultra turrax (see Fig. 2, left). During this process, the fibers were divided into smaller parts. The resulting suspension was treated in a high pressure homogenizer (see Fig. 2, right) by pumping with high velocities through fixed-geometry interaction chambers (Y or Z morphology) with diameters of 400, 200 and 75 μm. Through an E230Z$_{400 \mu m}$ and a H30Z$_{200 \mu m}$ chamber, the suspension passed for 13 times. Afterwards, the suspension cycled for 12 passes through an E230Z$_{400 \mu m}$ and a F20Y$_{75 \mu m}$ chamber, respectively. Pressures up to 1000 bar were applied to generate high shear-stresses to the cellulose fibers (Zimmermann et al. 2004). The concentration of resulting suspension was only 1.84% w/w or lower due to a high viscosity increase during the isolation procedure. Thus, in one 8-L batch, the dry content of cellulose was 80–150 g. Remarkably, dissimilar to untreated cellulose pulp fibers, the cationized fibers did not need the pre-treatment step in the inline disperser and could be processed directly in the high-shear homogenizer.

NFC films and composites with clay films preparation

A NFC 0.3% w/w suspension from mechanical disintegration process described above was filtered. In case of composite film preparation with clay, the NFC suspension was mixed with an aqueous 5% w/w clay slurry prior to filtration. The dewatered NFC

Fig. 2 Apparatus for cellulose disintegration, consisting of a reactor coupled to an inline disperser (*left*) and a high-shear homogenizer (*right*). **a** 10-L thermo-static reactor. **b** Ultra turrax. **c** Inline dispersing system. **d** Air pump. **e** Fixed-geometry interaction chambers (Y or Z morphology). **f** Container for NFC suspension

cakes (with and without clay) were then sandwiched between blotting-papers and dried in a hot press under loading of 15 MPa at 105 °C for 25 min.

Characterization

Elemental analysis

In order to obtain NFC powders from NFC suspensions (non-cationized NFC and TMA-NFC, respectively), these suspensions were dried in an oven at 40 °C with occasional stirring until powders were left. Subsequently, the powders were further dried in an oven overnight at 105 °C. Microelemental analyses of C, H, and N were performed by the microelemental laboratory of ETH Zürich on a LECO CHN-900 instrument (Leco Corporation, St. Joseph, MI, USA) for both non-cationized (starting material cellulose pulp and disintegrated materials) and TMA-NFC samples. Acetanilide and caffeine were used as calibration substances. The combustion products CO_2 and H_2O were analyzed quantitatively by infrared spectroscopy in order to determine the content of carbon and hydrogen, respectively, in the samples. Nitrogen (N_2) was determined by a thermal conductivity detector.

X-Ray photoelectron spectroscopy

The elements C, O, and N from non-modified and TMA-NFC films treated at 120 °C (see Table 1) were investigated with X-Ray photoelectron spectroscopy. Those films were produced by drying the suspensions of NFC on aluminium substrates in a vacuum drying oven overnight at 0.48 mbar and 40 °C.

The spectra were acquired on a Physical Electronics (PHI) Quantum 2000 photoelectron spectrometer using monochromated Al-Kα radiation generated from an electron beam operating at 15 kV and 25 W. The X-ray beam diameter on the sample specimen was 100 μm. Electrons photo-emitted from cellulose samples in ultra high vacuum (UHV) were collected and analyzed by a hemispherical capacitor electron-energy analyzer equipped with a channel plate and a position-sensitive detector. These electrons were discriminated based on their kinetic energy. The binding energy scale was calibrated for the Au 4f $_{7/2}$ electrons to be at 84.0 ± 0.1 eV. The electron take-off angle was 45° and the analyzer was operated in the constant pass energy mode of 117.4 eV (calibrated to a total

analyzer energy resolution of 1.62 eV for Ag 3d electrons) for survey scans. The detail scans of the C 1s, O 1s and N 1s signals were measured at an analyzer pass energy of 58.7 eV resulting in a spectrometer resolution of 1.05 eV. Compensation of surface charging during spectra acquisition was obtained by simultaneous operation of an electron and an argon ion neutralizer.

Analysis of the XPS spectra was performed using the MultiPak 6.1A software provided by the instruments manufacturer, Physical Electronics. A Shirley background subtraction was used to compute the peak intensities. The atomic concentrations were then calculated using the predefined sensitivity factors in the MultiPak 6.1A software.

In cellulose, the O 1s peaks are expected to be at 533.2 eV (Beamson and Briggs 1992). This energy shift was originating from slight sample surface charging, which was occurring during XPS analysis of electrically insulating samples. To compensate for this surface charging, the binding energies of all spectra were shifted (by about 2.7 eV) so that the O 1s signal is at 533.2 eV, the reference position for cellulose.

Methylene blue adsorption

Adsorption of methylene blue was carried out on starting material cellulose pulp powder and disintegrated material suspensions (non-modified NFC and TMA-NFC from reaction at 120 °C). In order to prevent the hornification during drying of suspension to powder form (Eyholzer et al. 2010; Tingaut et al. 2009) which would cause reduction of cellulose fibrils surface, the disintegrated material for this test was used in situ as suspension. In the experiments, 39 g of distilled water and 1 mL of methylene blue solution were added to 0.016 g of cellulose. The MB solution was prepared from 0.0163 g of MB (water content 15.5% w/w) in 100 mL of distilled water. In case of NFC suspension, the amount of added water was recalculated in order to maintain the same amount of water (39 g), cellulose (0.016 g) and methylene blue (1 mL) in all samples. The mixtures were then continuously shaken at 25 °C at 300 rpm for 24 h. The suspensions were afterwards centrifuged. After centrifugation, the optical absorbance of the supernatant liquids was measured in a CamSpec M302 spectrophotometer (Spectronic Camspec Ltd., United Kingdom) at a wavelength of $\lambda_{max} = 664$ nm, employing a 1 cm

polystyrene cuvette. Two replicates were performed for each type of sample. After 5 days, the measurements were repeated for all samples in order to assure that the adsorption process was complete.

X-ray diffraction

Cellulose pulp and disintegrated materials (non-modified NFC and TMA-NFC) in powder form (obtained from oven-drying as described in *Elemental Analysis*) were pressed to form pellets. The powder pellets were analyzed with a PANalytical (Almelo, Netherland) X' Pert Pro diffractometer. The diffractometer was equipped with a copper anode (Cu Kα) operating at a wavelength $\lambda = 1.5418$ Å. Cu Kα radiation was generated at 45 kV and 40 mA and a Ge (111) monochromator. All XRD spectra were recorded in the interval $5° < 2\theta < 40°$ with a step size of 0.033°. The reflected intensities were defined as functions of the diffraction angle 2θ.

The XRD patterns allowed the calculation of the crystallinity ratio (CR) (Segal et al. 1959; Thygesen et al. 2005; Buschlediller and Zeronian 1992):

$$CR = 1 - \frac{I_1}{I_2} \qquad (1)$$

where I_1 is the intensity of diffraction at the minimum between $2\theta = 18$ and 19° and I_2 the intensity of the crystalline peak at the maximum between $2\theta = 22$ and 23°.

Viscosity measurements

In general, the cellulose materials in powder form were dried in an oven for 24 h at 50 °C. A defined amount of cellulose material (m) was dissolved in cupriethylenediamine (CED) solution. The flow time of this mixture (t) through a marked distance of a capillary-tube viscometer was recorded. The intrinsic viscosity was calculated based on m and t parameters, according to ISO 5351 (2004) which has been used previously for the calculation of the degree of polymerization (DP) (Zimmermann et al. 2010). The intrinsic viscosity, $[\eta]$ (mL/g), is related to DP via the Staudinger–Mark–Houwink equation: $[\eta] = K \times DP^a$ where K and a depend on the polymer–solvent system. For cellulose dissolved in CED solution, two different regimes were found because of formation of superstructures at a DP of ca. 950 (Gruber and Gruber 1981). Accordingly,

$K = 2.28$ and $a = 0.76$ were determined for DP above ca. 950 and $K = 0.42$ and $a = 1$ for DP below ca. 950.

Scanning electron microscopy

Two different ways to prepare the samples for SEM investigations were employed. For sample preparation of the starting material, a small amount of dry cellulose pulp was sprinkled on carbon adhesive tape fixed on a specimen holder. For preparing samples of disintegrated materials, a drop of a diluted and ultra-turrax treated aqueous NFC suspension (0.05% w/w) was placed on a specimen holder. All samples were sputter-coated directly with a platinum layer of about 8 nm (BAL-TEC MED 020 Modular High Vacuum Coating Systems, BAL-TEC AG, Liechtenstein) in Ar as a carrier gas at 5×10^{-2} mbar. SEM was carried out using a FEI Nova NanoSEM 230 instrument (FEI, Hillsboro, Oregon, USA). SEM images were recorded with an accelerating voltage of 5 kV and a working distance of 5 mm.
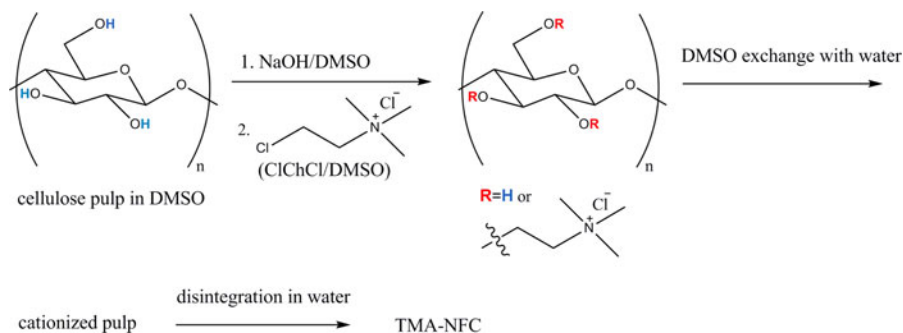
Results

Introduction of cationic groups into cellulose

The process of mechanical disintegration of native cellulose is described in the Experimental section. Modification of cellulose by reaction with chlorocholine chloride (ClChCl, Fig. 1) by Williamson ether synthesis was performed on cellulose pulp before disintegration, which is schematically depicted in Fig. 3. Note that the production of TMA-NFC was carried out without prior in-line dispersion process as required for disintegration of non-modified cellulose (see Experimental section) which saved energy and time.

The conversion of cellulose with ClChCl was performed in dimethyl sulfoxide (DMSO) as this solvent is appropriate for the Williamson ether synthesis (Smith et al. 1969). DMSO is a good (non-derivative) dispersing agent for cellulose and it does not hydrolyze ClChCl. Besides, DMSO can swell cellulose even two times better than water (Boluk 2005; Klemm et al. 2004). NaOH was added to convert alcohol groups of cellulose into more reactive alcoholate groups (note that water as a solvent would cause hydrolysis of chlorocholine chloride at alkaline conditions).

Fig. 3 Reaction scheme for the preparation of trimethylammonium-modified nanofibrillated cellulose (TMA-NFC) starting from cellulose pulp and chlorocholine chloride (ClChCl)

Characterizations of TMA-NFC

Elemental analysis

On the basis of elemental analyses, two reaction temperatures were selected at reaction times of 20 h for more detailed investigations: 97.5 °C, where the discolorations of the resulting materials were still weak (pale yellow) and 120 °C, where the resulting products were brown but the nitrogen content, indicative for the cellulose-bound ammonium groups, was considerably higher than after treatment at 97.5 °C (see Tables 1, 2).

Compared to other methods used for nitrogen analysis such as the Kjeldahl method (Schwarzinger et al. 2002) or dye adsorption (Abbott et al. 2006), microelemental analysis requires only small amounts of sample (<20 mg) and gives rather accurate results. Also, dye adsorption is only an indirect method for nitrogen analysis and therefore dependent on the reliability of the applied assumptions. Table 2 shows elemental analysis results of non-modified and modified cellulose samples. It is evident that the nitrogen contents

increased in the ClChCl treated samples statistically significant (95% confidence level) with increasing reaction temperature, implying the double quantity of ammonium groups per mass unit of cellulose in the samples modified at 120 °C compared to the samples modified 97.5 °C. The small quantity of nitrogen which appears in the non-modified samples was probably due to natural impurities (e.g. proteins, pectins or wax).

Theoretically, it is also possible to calculate the quantity of bound ammonium groups based on the content of the counter ion chloride (Hasani et al. 2008). Yet we found that the chloride content was not stable enough for the determination of the quantity of the chlorine. This could be due to (partial) exchange of chloride by hydroxide or other ions (impurities) during sample preparation or to the presence of extra chloride kept in fibers as metal salts which were hardly washed out.

X-ray photoelectron spectroscopy

In the XPS spectra, the intensity (or the number of electrons emitted and detected by the analyzer,

Table 2 Elemental analyses of starting material, non-modified NFC, and TMA-NFC prepared at 97.5 and 120 °C, respectively (reaction conditions see experimental section)

Sample	C (% w/w)	H (% w/w)	N (% w/w)	N/C (%)
Starting cellulose material[a]	42.97 ± 0.30	6.19 ± 0.18	0.05 ± 0.03	0.10
Non-modified NFC[b]	42.81 ± 2.56	6.17 ± 0.21	0.04 ± 0.00[e]	0.09
TMA-NFC (at T = 97.5 °C)[c]	43.07 ± 2.28	5.98 ± 0.23	0.13 ± 0.02	0.29
TMA-NFC (at T = 120 °C)[d]	44.33 ± 0.70	6.06 ± 0.09	0.27 ± 0.05	0.60

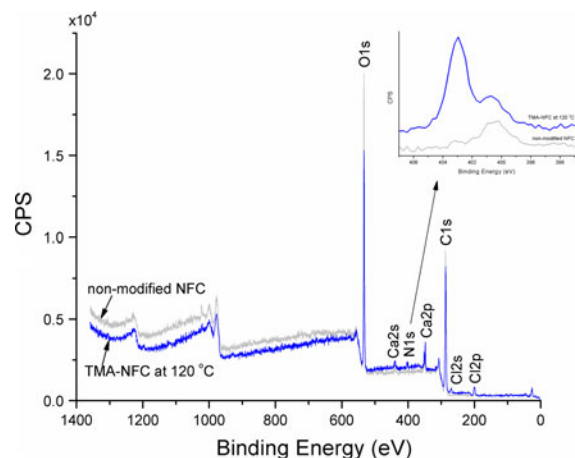Deviations are based on a 95% confidence level

[a] Mean value from 2 determinations of starting cellulose material

[b] Mean value from 4 determinations of non-modified NFC

[c] Mean value from 10 determinations of 5 different TMA-NFC samples prepared at a temperature of 97.5 °C

[d] Mean value from 10 determinations of 5 different TMA-NFC samples prepared at a temperature of 120 °C

[e] All four samples provided the same value (0.04% w/w)

Fig. 4 XPS survey spectra of non-modified NFC and TMA-NFC prepared at 120 °C. *Inset*: XPS detail spectra of the N 1s signal

Table 3 Atomic ratios of non-modified NFC and TMA-NFC prepared at 120 °C (two different analyses of one sample), evaluated from XPS after Shirley background subtraction

Sample	C/O	N/O
Non-modified NFC	1.73	0.005
TMA-NFC (at T = 120 °C)	1.94	0.045
TMA-NFC (at T = 120 °C)	1.86	0.047

been reported (Glaied et al. 2009; Montplaisir et al. 2008).

Table 3 shows atomic ratios C/O and N/O at the surface region of non-modified NFC and TMA-NFC evaluated from XPS detail scans. Generally the values of the two determinations of a TMA-NFC sample modified at a temperature of 120 °C were in good agreement and contained much more nitrogen at the surface region than the non-modified NFC samples, as expected when ammonium groups have been introduced. Assuming a H:O ratio of 2:1, as in cellulose, and neglecting the small amounts of detected calcium and chlorine, a nitrogen content of 1.6% w/w can be estimated in the surface region of the ClChCl exposed samples.

Methylene blue adsorption

Methylene blue (MB) is a cationic dye which was hypothesized to be adsorbed from aqueous phase on dispersed cellulose by interaction with –OH groups of cellulose via H-bonds (Kaewprasit et al. 1998). Accordingly, the MB adsorption capacities of different cellulose samples should represent the number of available surface –OH groups. Furthermore, it was assumed that the adsorption of MB (Blasutto et al. 1995; Kaewprasit et al. 1998; Abbott et al. 2006) should reflect the amount of cationic groups in cellulose since the cationic MB was supposed to be repelled when meeting the cationic groups of modified cellulose. It was then assumed that the degree of cationization can be determined on the basis that methylene blue is repelled by the cationic groups of modified cellulose.

Thus, we exposed various cellulose samples to methylene blue solutions, using always the same mass of cellulose and the same quantity of methylene blue (for details see "Experimental" section). The ratio of adsorbed methylene blue was calculated from the

respectively, in counts per second) is represented as a function of the binding energy (eV) these electrons had in the bulk. XPS survey spectra of non-modified NFC and TMA-NFC (Fig. 4) show intense O 1s signals at around 533.2 eV and an intense C 1s peak at around 286.7 eV. Ca peaks are observed in the spectra of both non-modified and TMA-NFC, which is common for natural celluloses derived from cotton or straw sources (Fras et al. 2005). In addition, in the spectrum of TMA-NFC, weak N and Cl signals emerge. The detection limit is below 1 atomic %.

The XPS detail scans of the N 1s peak of non-modified NFC and TMA-NFC prepared at 120 °C are illustrated in the inset of Fig. 4. The N 1s spectrum of NFC without modification shows a weak signal around 400.2 eV while the N 1s spectrum measured after the modification exhibits a dominating additional peak at higher binding energy (402.9 eV). This implies the presence of quaternary ammonium groups introduced into the cellulose by the reaction with ClChCl. For comparison, the measured binding energy of the N 1s electron is comparable to the N 1s position of 402.1 eV found in poly(4-vinylbenzyltrimethylammonium chloride) (Beamson and Briggs 1992). Notably, the C 1s and O 1s signals were charge-compensated so that the O 1s signal is at the reference position of cellulose (see *Experimental* section). Without charge-compensating, a N 1s position lower than 403 eV arisen for cationized cellulose containing other quaternary ammonium chloride groups have

concentration difference of methylene blue in the aqueous phase before and after adsorption, as measured by UV/Vis spectroscopy. The amount of adsorbed methylene blue on starting cellulose fibers, NFC (non-modified) and TMA-NFC (modified at 120 °C) amounted to 56, 45 and 31%, respectively. Since the adsorbed quantity of methylene blue is similar for cellulose fibers and NFC in spite of the manifold larger specific surface area of NFC, methylene blue cannot be suited to provide information on the outer surface of cellulose fibers, in contrast to opinions in the literature. It appears that methylene blue has access to the interior of a cellulose fiber due to swelling with water. The results are, however, compatible with the presence of cationic groups on TMA-NFC which repel methylene blue.

X-ray diffraction

XRD patterns of TMA-NFC, non-modified NFC and starting cellulose material (Fig. 5) always show four typical diffraction peaks of cellulose I at 2θ of 14.8, 16.6, 22.3, and 34.4°. These peaks correlate respectively with $1\bar{1}0$, 110, 020, and 004 lattice planes (Sassi and Chanzy 1995). A narrow peak at 22.3° (020) and a diffuse peak between 13 and 18° ($1\bar{1}0$, 110) reveal a quite high degree-of-order structure. The appearance of a small shoulder in the pattern of TMA-NFC at $2\theta = 20.6°$ on the lower side of the (020)-plane might indicate the presence of cellulose II (Moharram and
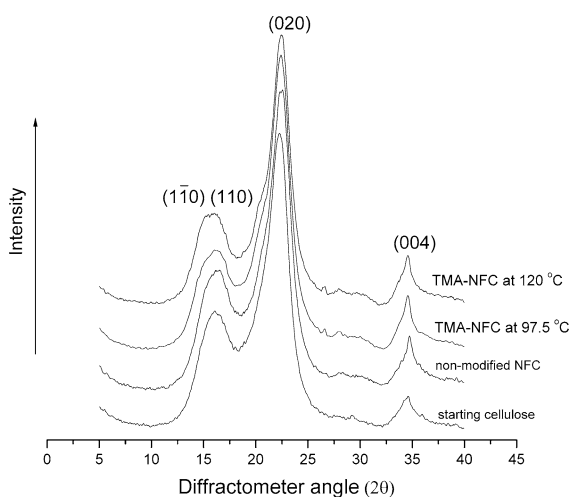
Table 4 Crystallinity ratios (CR) of cellulose pulp used as a starting material and disintegrated materials (non-cationized NFC and TMA-NFC), calculated from the intensity minimum I_1 and the intensity maximum I_2 of XRD patterns, see text

Sample	I_1	I_2	CR (%)
Starting cellulose material	2,849	9,627	70
Non-modified NFC	3,129	8,715	64
TMA-NFC (at T = 97.5 °C)	3,273	8,750	63
TMA-NFC (at T = 120 °C)	3,455	9,024	62

Mahmoud 2007). This shoulder can also be assigned to the (102)-plane (Thygesen et al. 2005; Sassi and Chanzy 1995).

The resulting crystallinity ratios calculation from XRD patterns (see *Experimental*) of starting cellulose material, non-modified and TMA-NFC samples are shown in Table 4. The crystallinity of the starting material (70%) was above that of the nanofibrillated celluloses including TMA-NFC (62–64%). Therefore, the impact of chemical modification on the crystallinity of the cellulose fibers was not significant, even for samples modified with ClChCl at 120 °C. In summary, the original pattern of cellulose I was clearly observed also in the TMA-NFC samples, indicating that most of the fiber crystalline structure was preserved.

Viscosity measurements

Viscosity measurements were used to estimate the degree of polymerization (DP) of cellulose samples. The DP values of starting cellulose material, non-modified NFC and TMA-NFC modified at two different temperatures are presented in Table 5. Obviously, the disintegration process did not affect the DP considerably as the values for cellulose fibers and NFC (non-modified) were similar. However, the chemical modification with ClChCl of cellulose led to a decrease of DP, which was more accentuated when the modification was performed at a temperature of 120 °C than at 97.5 °C.
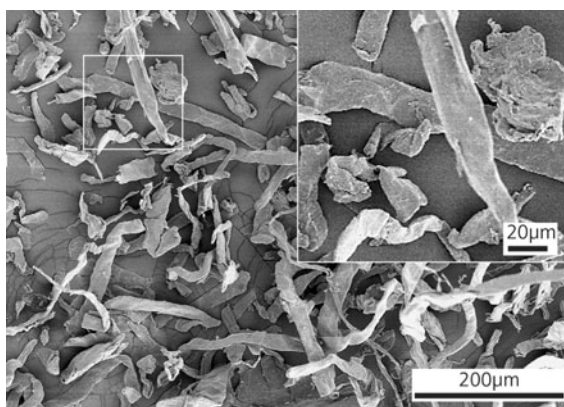
Scanning electron microscopy

The morphology of cellulose fibers before and after reaction with ClChCl was investigated with scanning electron microscopy (SEM). It is clearly evident from Figs. 6, 7, 8, 9 that the disintegration process was

Fig. 5 XRD spectra of starting cellulose material, non-modified NFC and TMA-NFC prepared at different temperatures

Table 5 Degrees of polymerization calculated from viscosity measurements of the starting material cellulose pulp and of disintegrated materials (non-modified NFC and TMA-NFC)
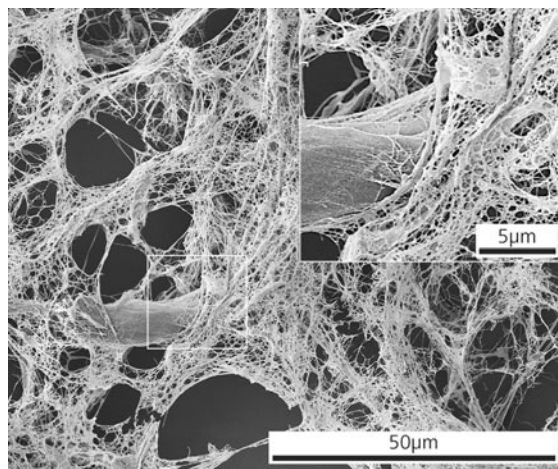
Sample	DP
Starting cellulose material	$1,494 \pm 52$
Non-modified NFC	$1,296 \pm 97$
TMA-NFC (at T = 97.5 °C)	718 ± 62
TMA-NFC (at T = 120 °C)	322 ± 7

The mean values are based on 3 determinations and the deviations on a 95% confidence level

successful since the structures in cellulose pulp are much coarser than those observed in the NFC samples. Figure 6 shows that the starting material, cellulose pulp, consists of fibers with typical diameters of 10–25 μm and lengths around 300 μm. While the fiber diameters of NFC could readily be measured, it was impossible to determine their lengths since the network structure of NFC was totally entangled. The diameters of ClChCl-treated and non-modified NFC fibrils lay typically in the range of ca. 50–100 nm (Figs. 7, 8, 9). Interestingly, TMA-NFC prepared at 120 °C provides a much finer and more homogeneous, uniform network structure compared to the non-modified NFC. The TMA-NFC prepared at 97.5 °C (Fig. 8) seems to have a less dense and less entangled network than TMA-NFC prepared at 120 °C (Fig. 9). In the latter case, the fibrils created quite even blocks or segments structures which are similar to foam structures. Finally, there was no indication for

Fig. 7 SEM micrograph of non-modified NFC. *Inset*: zoom-in image
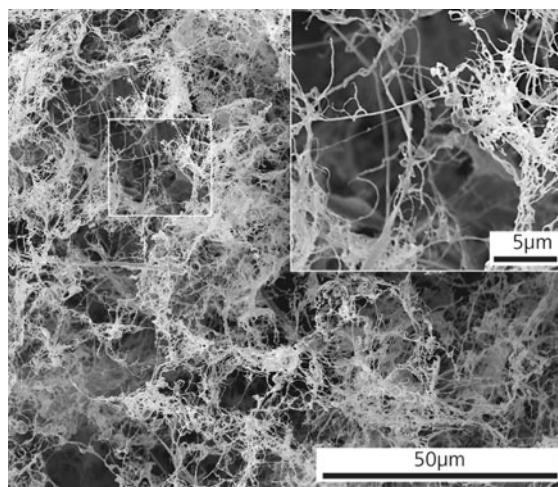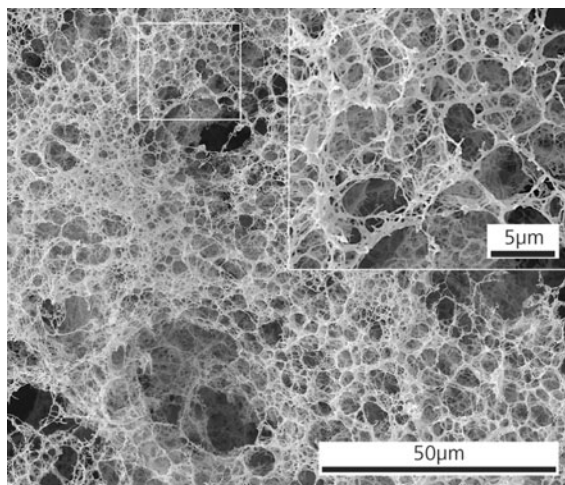

Fig. 8 SEM micrograph of TMA-NFC prepared at 97.5 °C. *Inset*: zoom-in image

pronounced degradation of NFC fibers by treatment with ClChCl.

Films of NFCs and NFC/Clay composite

Films of non-modified NFC and of TMA-NFC modified at 97.5 and 120 °C, respectively, were prepared by hot-pressing. Photographs of such films are shown in Fig. 10. The TMA-NFC films seem to be more transparent than the film with non-modified NFC, the latter showing clearly some opacity. Films with NFC modified at 97.5 °C are pale yellow while films with NFC modified at 120 °C are brownish but not opaque.

Fig. 6 SEM micrograph of cellulose pulp fibers used as starting material for the preparation of TMA-NFC. *Inset*: zoom-in image

Fig. 9 SEM micrograph of TMA-NFC prepared at 120 °C. *Inset*: zoom-in image

The dark colour of the film of TMA-NFC modified at 120 °C was probably a result of chromophore formation in cellulose by oxidation (Krainz et al. 2009), especially at high temperature in DMSO (Henniges et al. 2007); note that already a small fraction of chromophores can cause a pronounced colour.

Composite films of cellulose and 10% w/w montmorillonite were also prepared by the hot-pressing method. The composite films with clay are uniform

and still translucent (Fig. 11). Films modified with ClChCl appear more homogeneous to the eye than films of non-modified NFC, which are cloudy. This indicates that the clay is probably dispersed better in TMA-NFC than in non-modified NFC. The good dispersion of anionic silicate layers throughout the modified NFC network might be caused by ionic interactions between anionic clay layers and cationic groups in modified NFC.

Discussion

Cationic modification of NFC

Making use of ClChCl, the present study has highlighted a new approach for cationic-modified nanofibrillated cellulose production, which is basically applicable on an industrial scale.

In order to estimate the available fraction of surface hydroxyl groups of cellulose, we defined f as the ratio of surface hydroxyl groups to those in the bulk:
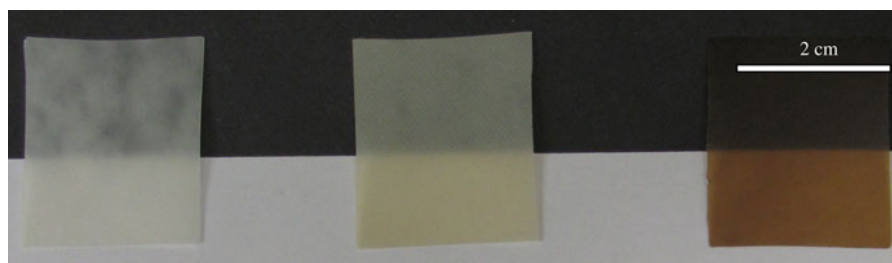
$$f = \frac{n_{-OH\,surface}}{n_{-OH\,bulk}} = \frac{\pi * (r + 2R)^2 - \pi * (r + R)^2}{\pi * (r + 2R)^2} \qquad (2)$$

For definitions of r and R compare Fig. 12, where r is the inner radius of the cellulose fiber or microfibril
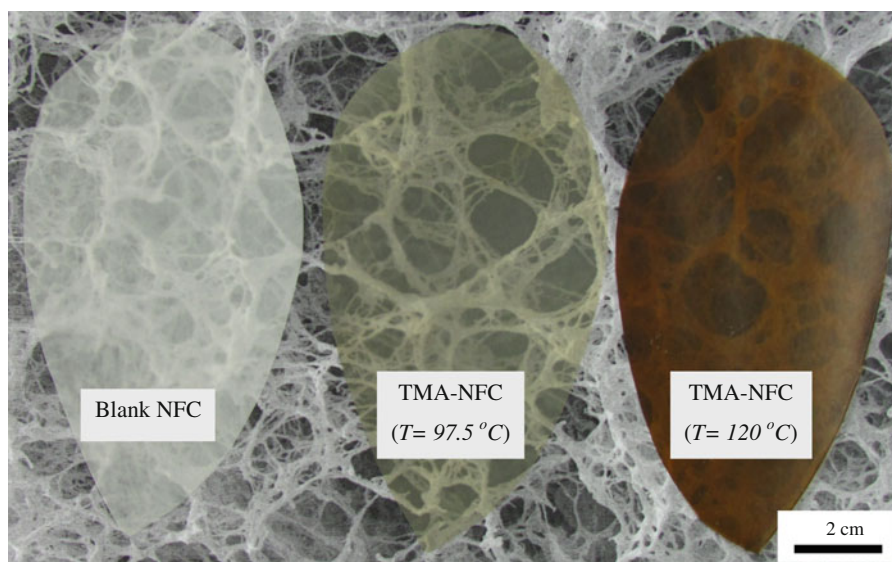

Fig. 10 From left to right: Photographs of films of non-modified NFC and TMA-NFC prepared at 97.5and 120 °C, respectively. The *scale bar* refers only to the films, not for the background

Fig. 11 Photographs of composite films containing 10% w/w montmorillonite and (from *left* to *right*) non-modified NFC, TMA-NFC prepared at 97.5 and at 120 °C, respectively

Fig. 12 Schematic illustration of the hierarchical structure of a cellulose fiber including a cross-section of a cellulose microfibril. A cross-section of a cellulose fiber can be expressed in the same way as for a cellulose microfibril, only with a different value of the radius r
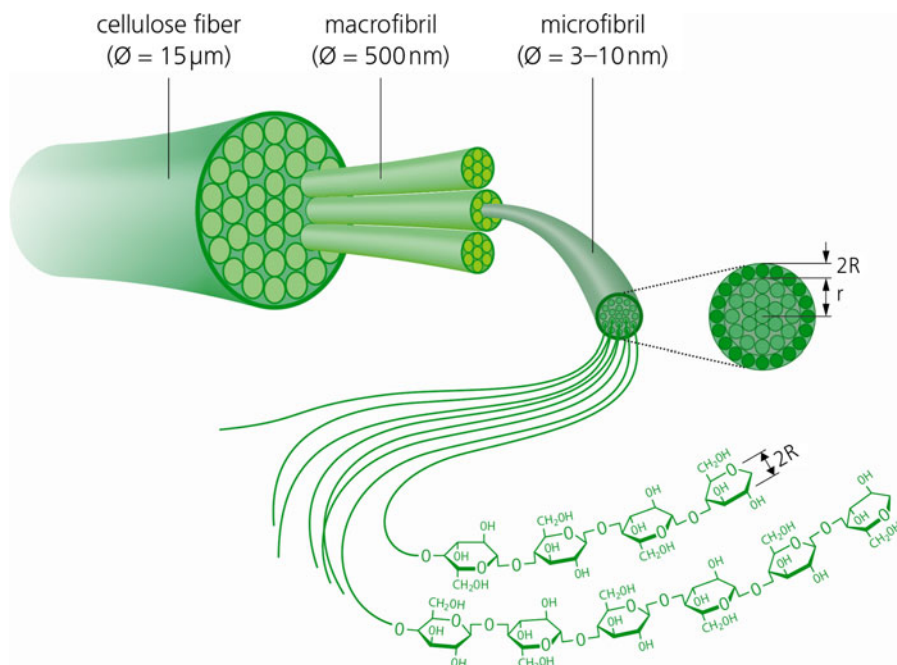
without the outer layer of glucose unit. The r values for fibers were derived from own morphological SEM investigations (Fig. 6), where the cellulose pulp fibers show diameters in the range of 10–25 μm. The values of r for microfibrils were taken from reported literature (Evert 2006). R is the radius of the glucose units on the surface of the fiber or fibril, with $R = 7.95 \times 10^{-10}$ m (Abbott et al. 2006).

Note that in formula (2), only a half of the –OH groups of the outer layer cellulose chains was assumed to be accessible for reaction. As evident from the schematic cross-section of a cellulose microfibril in Fig. 12, in 2 glucose molecules (one repeating unit of a cellulose chain), there are 3 hydroxyl groups on one and 3 on the opposite side of the molecules. Therefore, $(r + R)$ is the radius of the fiber or microfibril without

considering the surface of the outermost cellulose chains.

The cross-section of a cellulose fiber can be expressed in the same way as for a cellulose microfibril, only with a different value of r.

Thus in case of a fiber with radius $r = 7.5 \times 10^{-6}$ m, f becomes 2.12×10^{-4}. The molar amount of –OH groups in bulk cellulose, $n_{-OH\,bulk}$, is

$$n_{-OHbulk} = \frac{3 \times 1}{162.1406} = 0.0185 \, \text{mol/g}$$

where one glucose unit has three –OH groups and a molecular mass of 162.1406 g/mol.

Hence, the available quantity of –OH groups on the surface of cellulose fibers (possible swelling effect of the solvent neglected) is

$$n_{-\text{OHsurface}} = f \times n_{-\text{OHbulk}}$$
$$= 2.12 \times 10^{-4} \times 0.0185 \text{ mol/g}$$
$$= 3.9 \times 10^{-6} \text{mol/g}$$

If each surface –OH group of cellulose reacted with ClChCl, in 1 g cellulose, the maximum molar amount of trimethyl ammonium groups is 3.9×10^{-6} mol. This amount is equivalent to a maximum nitrogen content of N_{max} of 0.0055% w/w. This is, however, much less than the N contents of 0.13 and 0.27% found after reaction at 97.5 and 120 °C (see Table 2) which are 24 and 50 times higher than the estimated maximum nitrogen content at the fiber surface. Therefore, it appears that the swelling ability of DMSO (Boluk 2005; Klemm et al. 2004) enabled the reactants to enter inside the fiber and the reaction with ClChCl also took place at the surfaces of the fibrils.

When considering a microfibril with a radius $r = 5 \times 10^{-9}$ m (Evert 2006), $n_{-\text{OH surface}}$ becomes 4.2×10^{-3} mol/g, equivalent to N_{max} of 5.88% w/w. This value comes close to that estimated for the ammonium groups in the surface region by XPS, which amounted to around 1.6% w/w in the surface region. This indicates that the modification with ammonium groups indeed occurred predominantly at the surfaces of the microfibrils, at relatively high conversion of the fibrils' surface –OH groups.

The nitrogen contents (0.27% w/w in the bulk and 1.6% w/w in the surface region) are much higher than those reported for related modified cellulose fibers (Abbott et al. 2006), which were estimated on the basis of methylene blue adsorption. However, as indicated above in the section Results, quantitative calculations of surface –OH conversions at cellulose fibers by means of methylene blue adsorption have to be taken with care. Note in this context that methylene blue could also adsorb by exchange with cations (Shelden et al. 1993), e.g. with the calcium ions detected by XPS.

In a pre-test, modification of cellulose by reaction with ClChCl was also performed *after* disintegration. However, this method was less successful than modification before disintegration, apparently since the fibrils had been modified in situ with ammonium groups which caused repelling of the positively charged fibrils. This is in agreement with SEM images displaying cationized NFC fibrils with finer and more homogeneous fibril networks and less agglomerates than non-modifed NFC fibrils (Figs. 7, 8, 9).

Analogous results were reported for cellulose modified with anionic groups (Eyholzer et al. 2010). When two routes with interchanged sequence of carboxymethylation of cellulose and mechanical disintegration were applied, samples that were first carboxymethylated and then disintegrated provided better homogeneity and as a consequence better water-redispersibility. Probably, also in this case the electrostatic repulsion between fibrils of alike charges rendered the disintegration process more efficient (Wagberg et al. 2008; Eyholzer et al. 2010).

Degradation of TMA-NFC

The NFC itself (i.e. without ClChCl treatment) appears to undergo little degradation upon disintegration. The crystalline fraction and the degree of polymerization decreased only slightly (Table 4, 5). Yet the color changes (pale yellow and brown, respectively, for TMA-NFC prepared at 97.5 and 120 °C) indicate some degradation of cellulose under the action of the chemical treatment. However, as mentioned above, already small amounts of degradation products might cause pronounced colorations. The degree of polymerization (Table 5) became lower with increasing color intensity of the TMA-NFC. Under the applied modification conditions, a possible oxidation reaction with cellulose may take place through a chain "peeling" process causing a shortening in chain length. On the other hand, the crystallinity ratio of NFC did not change significantly upon chemical modification. No relevant relationships between crystallinity and degree of polymerization was also found in other reports (Shlieout et al. 2002). Finally, there was no evidence from SEM images (Figs. 7, 8, 9) or elemental analyses (Table 2) for massive degradation of cellulose, considering the confidence level of the elemental analyses and the fact that the carbon content of cellulose is expected to increase upon reaction with ClChCl. In summary, the above results show that degradation upon treatment with ClChCl resulted in materials which still can be attributed to the class of nanofibrillated cellulose.

The mechanical performance of TMA-NFC is expected not to be affected strikingly within the magnitude of the observed decrease in degree of polymerization (Zimmermann et al. 2010), since mechanical properties of NFC are related primarily to the network forming ability of NFC. This view is

supported by the preservation of the crystallinity ratio upon chemical modification (Iwamoto et al. 2007).

Films

Clays belong to the chemical class of layered silicates, whereat the thickness of the individual silicate layers amounts to the order of 1 nm. When the thickness of such particles embedded in a polymer matrix is well below the wavelength of light, the transmission of light or the translucence of the resulting films becomes higher. This is also the case when the cellulose units become finer. Therefore, because of the finer nanofibril dimensions of TMA-NFC (from SEM observations), non-modified NFC appeared more opaque to the eyes than TMA-NFC. In addition, TMA-NFC films were more homogeneous than films of non-modified NFC. With the addition of clay particles, the transparency of the materials decreased. In particular, the films with non-modified NFC became cloudy, in contrast to the films with TMA-NFC. This indicates the presence of clay agglomerates in the films based on non-modified NFC composites. In composite films of TMA-NFC, the clay appeared to be better dispersed; interactions between cationic groups in cationized NFC and the negatively charged clay surfaces might cause a dissociation of aggregates of clay and a good distribution of clay throughout the modified NFC network.

Conclusions

Nanofibrillated cellulose modified with quaternary ammonium groups (TMA-NFC) can be prepared by conversion of cellulose pulp with chlorocholine chloride (ClChCl), followed by a mechanical disintegration process. Due to swelling of the cellulose fibers by the solvent applied for the chemical reaction (DMSO), chlorocholine chloride had also access to the fibrils in the interior of the fibers, and a relatively high degree of surface –OH groups of the fibrils was converted. The degradation of cellulose induced by the chemical treatment was moderate, in spite of yellowish or brown discolorations of the resulting materials. The TMA-NFC showed a finer network structure and formed more transparent films than the non-modified materials. Also, clay (montmorillonite) dispersed better in

TMA-NFC than in non-modified nanofibrillated cellulose.

References

Abbott AP, Bell TJ, Handa S, Stoddart B (2006) Cationic functionalisation of cellulose using a choline based ionic liquid analogue. Green Chem 8(9):784–786

Alince B, Petlicki J, van de Ven TGM (1991) Kinetics of colloidal particle deposition on pulp fibers 1. Deposition of clay on fibers of opposite charge. Colloids Surf 59:265–277

Aulin C, Ahola S, Josefsson P, Nishino T, Hirose Y, Österberg M, Wagberg L (2009) Nanoscale cellulose films with different crystallinities and mesostructures—their surface properties and interaction with water. Langmuir 25(13): 7675–7685. doi:10.1021/la900323n

Azizi Samir MAS, Alloin F, Dufresne A (2005) Review of recent research into cellulosic whiskers, their properties and their application in nanocomposite field. Biomacromolecules 6(2):612–626. doi:10.1021/bm0493685

Beamson G, Briggs D (1992) High resolution XPS of organic polymers the Scienta ESCA300 database. Wiley, Chichester

Blasutto M, Delben F, Milost R, Painter TJ (1995) Novel cellulosic ethers with low degrees of substitution—I. Preparation and analysis of long-chain alkyl ethers. Carbohydr Polym 27(1):53–62

Bledzki AK, Gassan J (1999) Composites reinforced with cellulose based fibres. Prog Polym Sci 24(2):221–274

Boluk Y (2005) Acid–base interactions and swelling of cellulose fibers in organic liquids. Cellulose 12(6):577–593

Buschlediller G, Zeronian SH (1992) Enhancing the reactivity and strength of cotton fibers. J Appl Polym Sci 45(6): 967–979

Cai X, Riedl B, Ait-Kadi A (2003) Effect of surface-grafted ionic groups on the performance of cellulose-fiber-reinforced thermoplastic composites. J Polym Sci B Polym Phys 41(17):2022–2032

Cheng Q, Wang S, Rials T, Lee SH (2007) Physical and mechanical properties of polyvinyl alcohol and polypropylene composite materials reinforced with fibril aggregates isolated from regenerated cellulose fibers. Cellulose 14(6):593–602. doi:10.1007/s10570-007-9141-0

Daly S, Jachowicz J, Bianchini R (2010) Methods and kits containing charged compounds imparting benefits to hair and cosmetic products. WO10005906

de la Orden MU, González Sánchez C, González Quesada M, Martínez Urreaga J (2007) Novel polypropylene-cellulose composites using polyethylenimine as coupling agent. Compos Part A Appl Sci Manuf 38(9):2005–2012

Eichhorn S, Dufresne A, Aranguren M, Marcovich N, Capadona J, Rowan S, Weder C, Thielemans W, Roman M, Renneckar S, Gindl W, Veigel S, Keckes J, Yano H, Abe K, Nogi M, Nakagaito A, Mangalam A, Simonsen J, Benight A, Bismarck A, Berglund L, Peijs T (2010) Review: current international research into cellulose nanofibres and nanocomposites. J Mater Sci 45(1):1–33

Evert RF (2006) Esau's plant anatomy. Wiley, London

Eyholzer C, Bordeanu N, Lopez-Suevos F, Rentsch D, Zimmermann T, Oksman K (2010) Preparation and characterization of water-redispersible nanofibrillated cellulose in powder form. Cellulose 17(1):19–30

Fendler A, Villanueva M, Gimenez E, Lagarón J (2007) Characterization of the barrier properties of composites of HDPE and purified cellulose fibers. Cellulose 14(5):427–438

Fras L, Johansson LS, Stenius P, Laine J, Stana-Kleinschek K, Ribitsch V (2005) Analysis of the oxidation of cellulose fibres by titration and XPS. Colloids Surf A Physicochem Eng Asp 260(1–3):101–108

Glaied O, Dube M, Chabot B, Daneault C (2009) Synthesis of cationic polymer-grafted cellulose by aqueous ATRP. J Colloid Interface Sci 333(1):145–151. doi:10.1016/j.jcis.2009.01.050

Gruber E, Gruber R (1981) Viscosimetrical determination of the degree of polymerization of cellulose. Papier 35(4):133–141

Hasani M, Cranston ED, Westman G, Gray DG (2008) Cationic surface functionalization of cellulose nanocrystals. Soft Matter 4(11):2238–2244. doi:10.1039/b806789a

Henniges U, Kloser E, Patel A, Potthast A, Kosma P, Fischer M, Fischer K, Rosenau T (2007) Studies on DMSO-containing carbanilation mixtures: chemistry, oxidations and cellulose integrity. Cellulose 14(5):497–511

Hubbe MA, Rojas OJ, Lucia LA, Sain M (2008) Cellulosic nanocomposites: a review. BioResources 3(3):929–980

Iwamoto S, Nakagaito AN, Yano H, Nogi M (2005) Optically transparent composites reinforced with plant fiber-based nanofibers. Appl Phys Mater Sci Process 81(6):1109–1112

Iwamoto S, Nakagaito AN, Yano H (2007) Nano-fibrillation of pulp fibers for the processing of transparent nanocomposites. Appl Phys A Mater Sci Process 89(2):461–466

Kaewprasit C, Hequet E, Abidi N, Gourlot JP (1998) Application of methylene blue adsorption to cotton fiber specific surface area measurement: Part I. Methodology. J Cotton Sci 2:164–173

Klemm D, Philipp B, Heinze T, Heinze U, Wagenknecht W (2004) General considerations on structure and reactivity of cellulose: Section 2.2–2.2.3. In: Comprehensive cellulose chemistry. Wiley-VCH Verlag GmbH & Co. KGaA, pp 43–82. doi:10.1002/3527601929.ch2c

Krainz K, Potthast A, Suess U, Dietz T, Nimmerfroh N, Rosenau T (2009) Effects of selected key chromophores on cellulose integrity upon bleaching. Holzforschung, vol 63. De Gruyter. doi:10.1515/hf.2009.118

Moharram MA, Mahmoud OM (2007) X-ray diffraction methods in the study of the effect of microwave heating on the transformation of cellulose I into cellulose II during mercerization. vol 105. Wiley Subscription Services, Inc., A Wiley Company. doi:10.1002/app.26580

Montazer M, Malek R, Rahimi A (2007) Salt free reactive dyeing of cationized cotton. Fibers Polym 8(6):608–612

Montplaisir D, Daneault C, Chabot B (2008) Surface composition of grafted thermomechanical pulp through XPS measurement. BioResources 3(4):1118–1129

Nogi M, Handa K, Nakagaito AN, Yano H (2005) Optically transparent bionanofiber composites with low sensitivity to refractive index of the polymer matrix. Appl Phys Lett 87(24):243110–243113

Peffly MM, Geary NW, Staudigel JA (2004) Personal care composition containing a cationic cellulose polymer and an anionic surfactant system. WO04064802

Roy D, Knapp JS, Guthrie JT, Perrier S (2007) Antibacterial cellulose fiber via RAFT surface graft polymerization. Biomacromolecules 9(1):91–99. doi:10.1021/bm700849j

Sassi J-F, Chanzy H (1995) Ultrastructural aspects of the acetylation of cellulose. Cellulose 2(2):111–127. doi:10.1007/bf00816384

Schwarzinger C, Pfeifer A, Schmidt H (2002) Determination of the nitrogen content of cationic cellulose fibers by analytical pyrolysis. Monatshefte für Chemie/Chemical Monthly 133(1):1–7

Segal L, Creely JJ, Martin AE, Conrad CM (1959) An empirical method for estimating the degree of crystallinity of native cellulose using the X-ray diffractometer. Text Res J 29(10):786–794. doi:10.1177/004051755902901003

Shelden RA, Caseri WR, Suter UW (1993) Ion exchange on muscovite mica with ultrahigh specific surface area. J Colloid Interface Sci 157(2):318–327

Shlieout G, Arnold K, Müller G (2002) Powder and mechanical properties of microcrystalline cellulose with different degrees of polymerization. AAPS PharmSciTech 3(2):45–54. doi:10.1208/pt030211

Siqueira G, Bras J, Dufresne A (2009) Cellulose whiskers versus microfibrils: influence of the nature of the nanoparticle and its surface functionalization on the thermal and mechanical properties of nanocomposites. Biomacromolecules 0(0). doi:10.1021/bm801193d

Siró I, Plackett D (2010) Microfibrillated cellulose and new nanocomposite materials: a review. Cellulose. doi:10.1007/s10570-010-9405-y

Smith RG, Vanterpool A, Kulak HJ (1969) Dimethyl sulfoxide as a solvent in the Williamson ether synthesis. Can J Biochem Cell Biol 47(11):2015

Sorrentino A, Gorrasi G, Vittoria V (2007) Potential perspectives of bio-nanocomposites for food packaging applications. Trends Food Sci Technol 18(2):84–95

Stenstad P, Andresen M, Tanem B, Stenius P (2008) Chemical surface modifications of microfibrillated cellulose. Cellulose 15(1):35–45

Syverud K, Stenius P (2009) Strength and barrier properties of MFC films. Cellulose 16(1):75–85

Tanem BS, Kvien I, van Helvoort ATJ, Oksman K (2006) Morphology of cellulose and its nanocomposites. In: Cellulose nanocomposites. ACS Symposium Series. American Chemical Society, Washington, pp 48–62. doi:10.1021/bk-2006-0938.ch005

Thygesen A, Oddershede J, Lilholt H, Thomsen AB, Ståhl K (2005) On the determination of crystallinity and cellulose content in plant fibres. Cellulose 12(6):563–576. doi:10.1007/s10570-005-9001-8

Tingaut P, Zimmermann T, Lopez-Suevos F (2009) Synthesis and characterization of bionanocomposites with tunable properties from poly(lactic acid) and acetylated microfibrillated cellulose. Biomacromolecules 11(2):454–464. doi:10.1021/bm901186u

Turbak AF, Snyder FW, Sandberg KR (1983) Microfibrillated cellulose, a new cellulose product: properties, uses, and commercial potential. J Appl Polym Sci Symp 37:815–827

Wagberg L, Decher G, Norgren M, Lindstrom T, Ankerfors M, Axnas K (2008) The build-up of polyelectrolyte multilayers of microfibrillated cellulose and cationic polyelectrolytes. Langmuir 24(3):784–795. doi:10.1021/la702481v

Zimmermann T, Pöhler E, Geiger T (2004) Cellulose fibrils for polymer reinforcement. Adv Eng Mater 6(9):754–761

Zimmermann T, Pöhler E, Schwaller P (2005) Mechanical and morphological properties of cellulose fibril reinforced nanocomposites. Adv Eng Mater 7(12):1156–1161

Zimmermann T, Bordeanu N, Strub E (2010) Properties of nanofibrillated cellulose from different raw materials and its reinforcement potential. Carbohyd Polym 79(4): 1086–1093